NEUROSCIENCE

Neurogliaform cells dynamically decouple neuronal synchrony between brain areas

Ece Sakalar, Thomas Klausberger, Bálint Lasztóczi*

Effective communication across brain areas requires distributed neuronal networks to dynamically synchronize or decouple their ongoing activity. GABA*ergic* interneurons lock ensembles to network oscillations, but there remain questions regarding how synchrony is actively disengaged to allow for new communication partners. We recorded the activity of identified interneurons in the CA1 hippocampus of awake mice. Neurogliaform cells (NGFCs)—which provide GABA*ergic* inhibition to distal dendrites of pyramidal cells—strongly coupled their firing to those gamma oscillations synchronizing local networks with cortical inputs. Rather than strengthening such synchrony, action potentials of NGFCs decoupled pyramidal cell activity from cortical gamma oscillations but did not reduce their firing nor affect local oscillations. Thus, NGFCs regulate information transfer by temporarily disengaging the synchrony without decreasing the activity of communicating networks.

The brain is a complex system of networks interacting through concerted activity patterns broadcast through intricately structured connections (*1*, *2*). Rhythmic activation of neuronal assemblies in 10- to-30–ms time windows facilitates parsing of information by reader networks and generates transient gamma frequency (30 to 150 Hz) local field potential (LFP) oscillations (*3*–*5*). Gamma oscillations allow dynamic information routing (*6*, *7*) and neuronal circuits can perform active input selection if converging input pathways oscillate at different frequencies (*8*, *9*). However, many of the underlying brain mechanisms and network substrates remain unknown. In the hippocampus, sensory and mnemonic information from the entorhinal cortex and the CA3 area converge in the CA1 area (*10*) in which coordinated synaptic activity in terminals of temporoammonic (cortical) and Schaffer collateral (CA3) pathways give rise to mid-frequency ($gamma_M$; 75 Hz) and slow gamma oscillations ($gamma_S$; 37 Hz) in strata lacunosum-moleculare and radiatum, respectively (*11*–*13*). The association between afferent pathways and gamma oscillations paralleled by layer-specific arborizations of γ aminobutyric acid–expressing (GABA*ergic*) interneuron types make the rodent CA1 area a good candidate to explore input selection mechanisms (*14*, *15*).

We reasoned that activity of CA1 cells regulating cortico-hippocampal information flow would follow the dynamics of temporoammonic pathway that manifests as $gamma_M$ (*6*, *11*–*13*). To discover such neurons we simultaneously recorded layer-dependent gamma oscillations and neuronal spike timing in the dorsal hippocampal CA1 area of head-restrained mice running in a virtual corridor for a water reward (fig. S1) (*16*). To study $gamma_M$, $gamma_S$, and locally generated fast gamma oscillations ($gamma_F$; 120 Hz) (*12*) in isolation, volume-conducted LFP components were suppressed by calculating current source density (CSD; fig. S2) (*5*, *13*, *16*). Spike timing of most (84%) GABA*ergic* cells in CA1 ($n = 336$ cells) depended only weakly or not at all ($r < 0.07$) on the phase of $gamma_M$. However, a small neuron population (7.4%)—almost entirely located in stratum lacunosum-moleculare (23 of 25 cells)—showed distinctively strong phase locking ($r > 0.14$; Fig. 1 and fig. S3, supplementary text). Stratum lacunosum-moleculare also contained cells with little ($n = 22$) or no ($n = 28$) modulation by $gamma_M$ (Fig. 1C and fig. S3E). To identify the cells that fire phase locked to $gamma_M$ we labeled recorded cells with neurobiotin for post hoc histological analysis (*16*). Out of six successfully labeled stratum lacunosum-moleculare neurons, five showed strong coupling to $gamma_M$ with phase preference indistinguishable from other strongly coupled cells of this layer (Fig. 1, B to D; $P = 0.8$, Watson-Williams test; $n = 18$ cells). All five cells were identified as neurogliaform cells (NGFCs) (Fig. 1A and table S1, supplementary text). The spike timing of the sixth neuron was independent of $gamma_M$ ($P = 0.31$, Rayleigh test; $n = 297$ spikes), and this cell was not a NGFC (fig. S4; tables S1 and S2). Thus the population of GABA*ergic* stratum lacunosum-moleculare neurons with strong ($r = 0.27 \pm 0.07$) preferential firing on $gamma_M$ troughs ($\mu = 5.3 \pm 17.1°$; $n = 23$) corresponds to NGFCs (fig. S5; supplementary text). Firing of NGFCs was not coupled to $gamma_F$ and showed variable phase modulation by $gamma_S$ (figs. S6 and S7 and table S2). Oriens lacunosum-moleculare (OLM) cells also provide GABA*ergic* innervation to stratum lacunosum-moleculare but their soma and dendrites are located in stratum oriens (*14*). Spike timing of OLM cells was independent of $gamma_M$ but was moderately modulated by $gamma_F$ (fig. S8).

In awake rodents, 5 to 12 Hz theta oscillations occur during movement and irregular activity with intermittent sharp-wave ripple complexes (SWR) prevails during rest (Fig. 2A). The occurrence of SWRs had no effect on NGFC firing rate (fig. S9) (*17*), which markedly increased during theta oscillations (from 3.4 ± 3.9 Hz to 7.4 ± 4.7 Hz, $P = 4.6 \times 10^{-5}$, Wilcoxon signed-rank test; $n = 23$ cells; Fig. 2, A and B). Firing of some putative pyramidal cells (place cells) was restricted to sections of the corridor (place fields) and was phase precessing from ascending phase to peak of theta during traversals (Fig. 2 and fig. S10) (*18*). By contrast, NGFCs ($n = 16$, 2 identified and 14 putative) showed minimal spatial selectivity and constant theta phase preference (Fig. 2, A, C, and D, and fig. S10). Consequently, place cell spikes coincided with NGFC firing mostly on theta peaks upon place field exit (Fig. 2D and fig. S10A), when place cell firing is maximally modulated by $gamma_M$ (*13*, *19*).

Multisite recordings along the transverse axis of CA1 (fig. S11) disclosed widespread, tight, zero-lag phase synchrony and more spatially restricted amplitude correlations of $gamma_M$ (fig. S12, supplementary text). NGFCs fired on peaks of theta cycles ($r = 0.54 \pm 0.15$; $\mu = 206 \pm 18°$; $n = 23$) (*17*), coincident with high-amplitude $gamma_M$ ($r = 0.19 \pm 0.04$; $\mu = 193 \pm 8°$; $n = 63$ experiments) (*12*, *13*, *19*) implicating temporoammonic pathway $gamma_M$ synchrony in NGFC recruitment (Fig. 3A, fig. S13, and table S2). Indeed, within theta cycles NGFCs started to fire in high-amplitude $gamma_M$ cycles [Fig. 3B; $P = 6.8 \times 10^{-22}$; repeated measures one-way analysis of variance (ANOVA); $n = 23$]. To understand the consequences of NGFC activation we simulated the inhibitory postsynaptic $GABA_A$ conductance trace (g_{syn}) for NGFC spike trains (fig. S14). Because of its slow kinetics (*20*, *21*) NGFC-driven $GABA_A$ receptor-dependent inhibition may last for several $gamma_M$ cycles after the spike (fig. S14). This inhibition did not desynchronize $gamma_M$ per se as $gamma_M$ amplitude remained elevated after NGFC firing commenced (Fig. 3B). NGFCs may regulate cortico-hippocampal communication by releasing GABA onto apical dendritic tufts of CA1 pyramidal cells. In theta cycles, $gamma_M$ phase modulation of pyramidal cells first strengthened with the increasing $gamma_M$ amplitude (Fig. 3A and fig. S15A; $P = 2 \times 10^{-29}$; ANOVA with Tukey-Kramer correction; $n = 32$ experiments) but peaked earlier ($r = 0.21 \pm 0.08$; $\mu = 167 \pm 25°$; $n = 32$), conspicuously dropping as NGFC-dependent inhibition emerged phase-shifted by a quarter theta cycle from NGFC firing ($\mu = 288 \pm 18°$; $n = 23$; Fig. 3A). During the buildup of NGFC-dependent inhibition, pyramidal cell firing ramped (Fig. 3A). Pyramidal cell silencing after NGFC activation was not indicated in analysis of either cross correlograms (fig. S15,

Division of Cognitive Neurobiology, Center for Brain Research, Medical University of Vienna, Vienna, Austria.
*Corresponding author. Email: balint.lasztoczi@meduniwien.ac.at

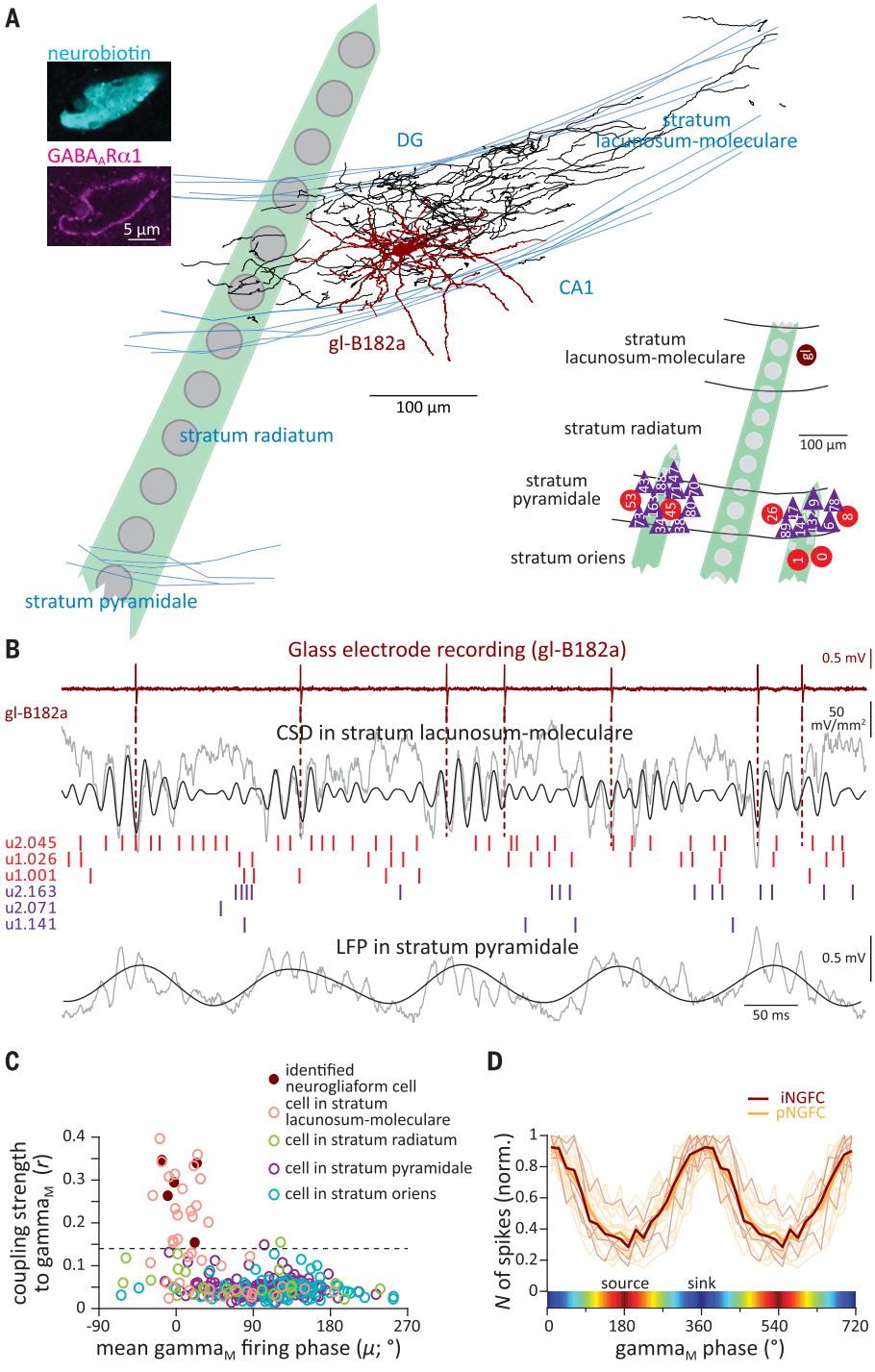

Fig. 1. NGFCs in the hippocampal CA1 area show distinctly strong coupling to mid-frequency gamma oscillations. (**A**) Reconstruction of somatodendritic (dark red) and axonal (black) arbors of cell gl-B182a recorded and labeled in experiment B182a and confocal scans showing the neurobiotin-labeled cell gl-ES9b (cyan) and GABA$_A$Rα1 subunit immunoreactivity (magenta). Cells gl-B182a and gl-ES9b were identified as NGFCs. (Inset) Schematic locations of putative GABA*ergic* (red circles) and pyramidal cells (purple triangles), and the cell gl-B182a recorded by the glass electrode (dark red circle) in experiment B182a. (**B**) Spike timing of neuron gl-B182a (dark red) and of other putative GABA*ergic* (red) and pyramidal cells (purple), together with gamma$_M$ (CSD in stratum lacunosum-moleculare, 53 to 90 Hz) and theta oscillations (LFP in stratum pyramidale, 5 to 12 Hz) in experiment B182a (gray, unfiltered traces). (**C**) Scatter plot of coupling strength versus preferred firing phase of all CA1 GABA*ergic* cells significantly coupled to gamma$_M$ (n = 262 cells). Estimated soma locations are color-coded; filled dark red circles represent identified NGFCs. Dotted line indicates threshold for strong coupling (0.14). (**D**) Distribution of spike counts of identified (iNGFC; dark red) and putative (pNGFC; orange) NGFCs as a function of gamma$_M$ phase (normalized to maxima; thick lines, mean).

C and D) or spike counts in gamma$_M$ cycles (Fig. 3B). To more directly probe the decoupling of CA1 from cortical inputs by NGFCs we compared phase coupling of pyramidal cell spikes in gamma$_M$ cycles before and after NGFC spikes. Immediately after the gamma$_M$ cycle hosting the first NGFC spike in a theta cycle, the coupling strength of pyramidal cell firing dropped (Fig. 3B and fig. S15E; $P = 1.1 \times 10^{-5}$; ANOVA with Tukey-Kramer correction; n = 14 experiments) and became largely not significant (fig. S16, A to C; α = 0.05; Rayleigh test), an effect specific to gamma$_M$ (fig. S16) and NGFCs (fig. S17). Although within gamma$_M$ cycles NGFCs fired 90° (3.3 ms) before pyramidal cells (Fig. 3C; n = 241 cells; r = 0.054 ± 0.021; μ = 98 ± 28° for pyramidal cells), in the cycle of the first NGFC spike the slow onset of inhibition permitted efficient cortico-hippocampal communication and therefore gamma$_M$ coupling of pyramidal cells remained elevated (Fig. 3B and fig. S17C). Decoupling was not a mere consequence of theta phase comodulation of NGFC firing, pyramidal cell gamma$_M$ coupling, and gamma$_M$ but instead depended on NGFC spike timing itself (figs. S18 and S19, supplementary text). Firing of putative GABA*ergic* cells in stratum pyramidale but not in stratum oriens also abruptly decoupled from gamma$_M$ oscillations after NGFC spikes (fig. S20). Thus, after NGFC activation the CA1 circuit decouples from cortical afferents (Fig. 3D).

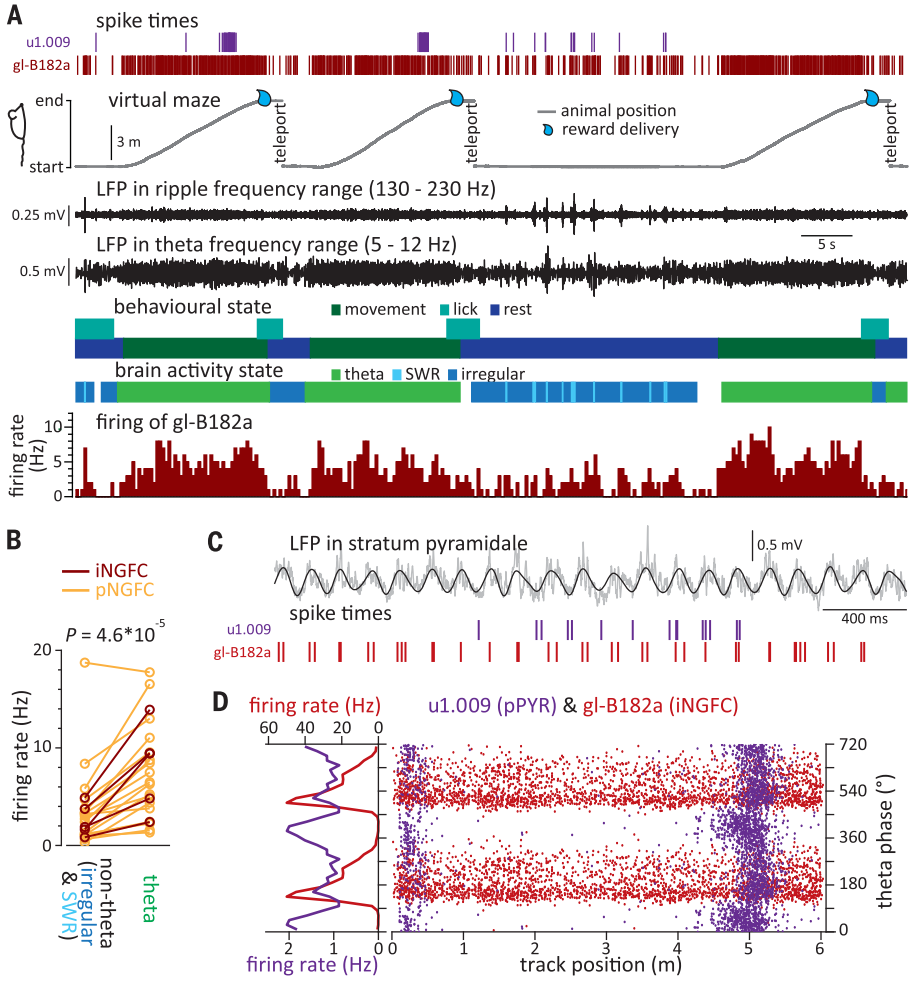

Fig. 2. NGFCs are activated during theta oscillations. (**A**) Spike times of an identified NGFC (gl-B182a; dark red) and putative pyramidal cell (u1.009, a place cell; purple) during three runs on the virtual corridor, together with ripple and theta oscillations from stratum pyramidale. Behavioral and brain states are indicated by color-coded boxes. Lower plot: Firing rate of cell gl-B182a in 300-ms windows. (**B**) Comparison of NGFC firing rates during theta versus nontheta periods. (**C**) Spike times of cells in (A) on an expanded time scale as the animal walks through the place field of u1.009, together with theta oscillations (5 to 12 Hz LFP in stratum pyramidale; gray, unfiltered trace). (**D**) Theta phase versus position raster plot of spikes of gl-B182a (dark red) and u1.009 (phase precessing place cell, purple). (Left) Theta phase dependence of the firing rates.

We discovered a network mechanism for dynamic regulation of cortico-hippocampal information transfer in the CA1 area. NGFCs release GABA to stratum lacunosum-moleculare, inducing slow inhibition in all pyramidal cell apical dendritic tufts within their axonal arbor (*20*–*22*). The faster $GABA_A$ component of this indiscriminate, layer-specific inhibition mediated by unitary volume transmission disconnects pyramidal cells from cortical afferents for a fraction of a theta cycle reported by a temporary decoupling of their spike timing from $gamma_M$ after NGFC firing. Summating over several theta cycles $GABA_B$ receptor mediated processes may regulate inputs on behavioral time scales (*14*, *20*, *22*). Cortical afferents contribute little to pyramidal cell firing rates but are indispensable for intact temporal organization and place fields in CA1 (*23*). This explains maintained pyramidal cell firing despite reduced cortico-hippocampal communication. The distal location of cortical synapses limits their influence (*24*) and therefore modulation of CA1 pyramidal cell firing by $gamma_M$ is generally weak (*12*, *13*). Cortico-hippocampal information transfer and coupling to $gamma_M$ can strengthen with cognitive load (*25*, *26*) during some network operations (*13*, *26*–*28*) and pathway interactions (*24*, *27*, *29*), implying dynamic control; inhibition by NGFCs provides a mechanism to exercise such control. Thalamic afferents also target NGFCs (*30*), further increasing the versatility of this cell type.

During exploration theta oscillations organize hippocampal activity, modulate gamma oscillation amplitudes (*11*–*13*, *31*), and segment pyramidal cell firing sequences (*32*). On theta peaks, activity and $gamma_M$ synchrony build up in the temporoammonic pathway and give rise to $gamma_M$ in stratum lacunosum-moleculare (*12*, *31*), which entrains CA1 pyramidal cell spikes when theta firing sequences start (*13*). This waxing rhythmic excitation also induces spiking in NGFCs with a lag (*22*), first when the amplitude of $gamma_M$ is already high. Late spiking and slowly rising postsynaptic currents of NGFCs ensure a window of efficient cortico-hippocampal information transfer before NGFCs detune pyramidal cells from $gamma_M$, allowing other pathways to control pyramidal cell recruitment to theta sequences (*13*). Thus NGFCs minimize input interference and optimize conditions for cooperative synaptic plasticity (*24*, *27*, *29*). Waning cortical excitation (*31*) and waxing inhibition from OLM cells (*33*–*35*) silence NGFCs on theta troughs, which prepares the network for the next cycle of $gamma_M$ synchronization through recovering the dynamic range of inhibition.

Neurogliaform cells are key regulators of cortical information flow to CA1, orchestrating precise integration of sensory and mnemonic information. Fast-spiking GABA*ergic* cells facilitate cortical communication by conducting gamma oscillations (*14*, *36*, *37*). By contrast, NGFCs with input layer-associated axonal and dendritic arbors, ubiquitous in cortical circuits (*22*, *38*, *39*), detune principal cell firing and regulate information flow by afferent-specific decoupling.

REFERENCES AND NOTES

1. S. W. Oh *et al.*, *Nature* **508**, 207–214 (2014).
2. A. Pouget, P. Dayan, R. Zemel, *Nat. Rev. Neurosci.* **1**, 125–132 (2000).
3. G. Buzsáki, *Neuron* **68**, 362–385 (2010).
4. P. Fries, *Neuron* **88**, 220–235 (2015).
5. B. Pesaran *et al.*, *Nat. Neurosci.* **21**, 903–919 (2018).

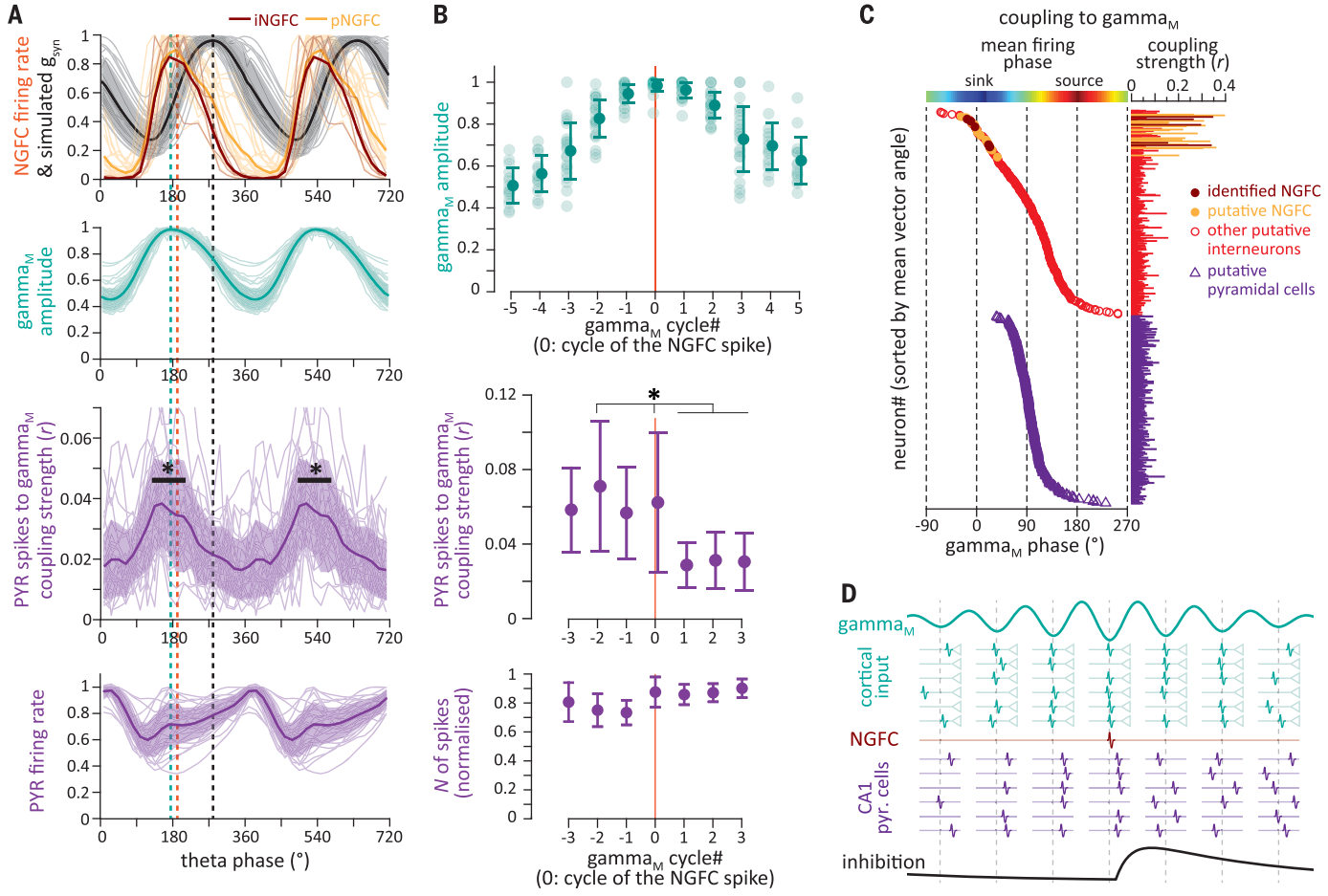

Fig. 3. Action potentials of NGFCs decouple pyramidal cell firing from mid-frequency gamma oscillations but do not suppress their activity. (**A**) Theta phase modulation of NGFC firing rate (dark red and orange for identified and putative NGFCs, respectively; normalized) and the simulated resultant inhibitory postsynaptic conductance in pyramidal cells (g_{syn}; black; normalized); of gamma$_M$ amplitude (normalized, turquoise); of coupling strength of pyramidal cell firing to gamma$_M$ (purple); and of pyramidal cell activity (purple, normalized). Light lines indicate individual experiments (pyramidal cells pooled); thick lines and shading indicate mean ± SD; asterisk, significant enhancement (α = 0.05, ANOVA with Tukey-Kramer correction). (**B**) Amplitude of gamma$_M$ (normalized, turquoise), and phase-coupling strength (r, purple, middle) and number (purple, bottom) of pyramidal cell spikes in gamma$_M$ cycles before (cycle number < 0), after (cycle number > 0) and during (cycle 0) the first NGFC spike in a theta cycle (asterisks indicate P < 0.05, ANOVA with Tukey-Kramer correction). (**C**) Mean firing phase (μ) and coupling strength (r) of identified (dark red) and putative (orange) NGFCs, other GABA*ergic* cells (red) and pyramidal cells (purple triangles) ordered by the mean firing phase (only cells significantly modulated by gamma$_M$ are plotted). (**D**) Schematic illustration of how NGFC activation affects cortico-hippocampal communication through gamma$_M$ oscillations.

6. T. Akam, D. M. Kullmann, *Neuron* **67**, 308–320 (2010).
7. G. G. Gregoriou, S. J. Gotts, H. Zhou, R. Desimone, *Science* **324**, 1207–1210 (2009).
8. A. Palmigiano, T. Geisel, F. Wolf, D. Battaglia, *Nat. Neurosci.* **20**, 1014–1022 (2017).
9. A. Fernández-Ruiz *et al*., *Science* **372**, eabf3119 (2021).
10. N. M. van Strien, N. L. Cappaert, M. P. Witter, *Nat. Rev. Neurosci.* **10**, 272–282 (2009).
11. L. L. Colgin *et al*., *Nature* **462**, 353–357 (2009).
12. E. W. Schomburg *et al*., *Neuron* **84**, 470–485 (2014).
13. B. Lasztóczi, T. Klausberger, *Neuron* **91**, 34–40 (2016).
14. K. A. Pelkey *et al*., *Physiol. Rev.* **97**, 1619–1747 (2017).
15. T. P. Vogels, L. F. Abbott, *Nat. Neurosci.* **12**, 483–491 (2009).
16. Materials and methods are available as supplementary materials.
17. P. Fuentealba *et al*., *J. Neurosci.* **30**, 1595–1609 (2010).
18. J. O'Keefe, M. L. Recce, *Hippocampus* **3**, 317–330 (1993).
19. M. Guardamagna, F. Stella, F. P. Battaglia, bioRxiv 2021.12.22.473863v1 [Preprint] (2021); https://doi.org/10.1101/2021.12.22.473863.
20. C. J. Price, R. Scott, D. A. Rusakov, M. Capogna, *J. Neurosci.* **28**, 6974–6982 (2008).
21. S. Oláh *et al*., *Nature* **461**, 1278–1281 (2009).
22. L. Overstreet-Wadiche, C. J. McBain, *Nat. Rev. Neurosci.* **16**, 458–468 (2015).
23. M. I. Schlesiger *et al*., *Nat. Neurosci.* **18**, 1123–1132 (2015).
24. T. Jarsky, A. Roxin, W. L. Kath, N. Spruston, *Nat. Neurosci.* **8**, 1667–1676 (2005).
25. V. Lopes-dos-Santos *et al*., *Neuron* **100**, 940–952.e7 (2018).
26. A. Fernández-Ruiz *et al*., *Neuron* **93**, 1213–1226.e5 (2017).
27. K. C. Bittner *et al*., *Nat. Neurosci.* **18**, 1133–1142 (2015).
28. H. O. Cabral *et al*., *Neuron* **81**, 402–415 (2014).
29. M. Remondes, E. M. Schuman, *Nature* **416**, 736–740 (2002).
30. R. Chittajallu *et al*., *Nat. Commun.* **8**, 152 (2017).
31. K. Mizuseki, A. Sirota, E. Pastalkova, G. Buzsáki, *Neuron* **64**, 267–280 (2009).
32. W. E. Skaggs, B. L. McNaughton, M. A. Wilson, C. A. Barnes, *Hippocampus* **6**, 149–172 (1996).
33. D. Elfant, B. Z. Pál, N. Emptage, M. Capogna, *Eur. J. Neurosci.* **27**, 104–113 (2008).
34. C. Varga, P. Golshani, I. Soltesz, *Proc. Natl. Acad. Sci. U.S.A.* **109**, E2726–E2734 (2012).
35. L. Katona *et al*., *Neuron* **82**, 872–886 (2014).
36. J. A. Cardin *et al*., *Nature* **459**, 663–667 (2009).
37. B. V. Atallah, M. Scanziani, *Neuron* **62**, 566–577 (2009).
38. B. Schuman *et al*., *J. Neurosci.* **39**, 125–139 (2019).
39. X. Jiang *et al*., *Science* **350**, aac9462 (2015).
40. E. Sakalar, Zenodo (2022); https://doi.org/10.5281/zenodo.6580307.

ACKNOWLEDGMENTS

We thank A. Wallerus for his help with creating the flat maps of the stratum lacunosum-moleculare (including creating and sharing software) and for his help with cell reconstruction and histological processing. The technical assistance of R. Hauer, M. S. Mateos, and E. Dögl is highly appreciated. We thank A. Wallerus, I. Vörösházy, and A. Leonhartsberger for training some of the animals and I. Vörösházy for performing some of the recordings. We thank P. Scholze for providing us with the experimental subjects and P. Scholze and W. Sieghart for their generous gift of antibodies against the α1 and δ subunits of the GABA$_A$ receptor. **Funding:** This work was supported by the FWF Austrian Science Fund, Stand-Alone Project P-29744-B27 (to B.L.). **Author contributions:** Conceptualization: B.L., E.S., and T.K. Methodology: B.L., E.S., and T.K. Investigation: E.S. and B.L. Formal analysis: E.S. and B.L. Software: B.L. and E.S. Data curation: E.S., B.L., and T.K. Visualization: E.S., B.L., and T.K.

Funding acquisition: B.L. and T.K. Project administration: B.L., T.K., and E.S. Supervision: B.L. and T.K. Writing – original draft: E.S. and B.L. Writing – review and editing: E.S., B.L., and T.K. **Competing interests:** The authors declare that they have no competing interests. **Data and materials availability:** All data are available in the manuscript and supplementary materials. Custom MATLAB scripts can be downloaded from (*40*). **License information:**

SUPPLEMENTARY MATERIALS

View/request a protocol for this paper from *Bio-protocol*.

Submitted 27 January 2022; accepted 30 May 2022
10.1126/science.abo3355

Neurogliaform cells dynamically decouple neuronal synchrony between brain areas

Ece SakalarThomas KlausbergerBálint Lasztóczi

Science, 377 (6603), • DOI: 10.1126/science.abo3355

Fine-tuning information transfer

To generate adaptive behavior, our brains constantly combine information from multiple sources. How do neuronal circuits orchestrate and maintain the balance of different input streams in the face of constant change? Sakalar *et al*. discovered that neurogliaform cells were strongly coupled with gamma oscillations that are associated with gating the interaction of hippocampus and cortex (see the Perspective by Craig and Witton). The activity of neurogliaform cells was correlated with a decrease in coupling between pyramidal cell firing and gamma oscillations without affecting the overall levels of activity of the pyramidal cells. Neurogliaform cells locally released the neurotransmitter #-aminobutyric acid, which selectively decreased the influence of neocortical inputs to hippocampal area CA1 at specific stages in the local field potential. This modulation of inputs allows for the transfer of different types of information at different times. —PRS